Am J Transl Res 2016;8(3):1397-1411
www.ajtr.org /ISSN:1943-8141/AJTR0022262

Original Article

Early protective role of MST1 knockdown in response to experimental diabetic nephropathy

Weihua Wu[1*], Maoping Zhang[2*], Santao Ou[1], Xing Liu[3], Ling Xue[4], Jian Liu[1], Yuke Wu[5], Ying Li[1], Qi Liu[1]

[1]Department of Nephrology, The Affiliated Hospital of Southwest Medical University, China; [2]Department of Nephrology, The Traditional Chinese Medical Hospital of Southwest Medical University, China; [3]Department of Cardiology, The Affiliated Hospital of Southwest Medical University, China; [4]Department of Urology Surgery, The Affiliated Hospital of Southwest Medical University, China; [5]Department of Ophthalmology, The Traditional Chinese Medical Hospital of Southwest Medical University, China. [*]Equal contributors.

Received December 19, 2015; Accepted February 19, 2016; Epub March 15, 2016; Published March 30, 2016

Abstract: Diabetic nephropathy (DN) is a progressive kidney disease caused by the damage of capillaries in kidney's glomeruli. Mammalian Sterile 20-like kinase 1 (MST1) has been reported to play an important role in many disease, such as diabetes, cardiac disease and ect. However, the potential role of MST1 pathway in DN has not been fully evaluated. In this study, we hypothesized that MST1 could be involved in DN, and MST1 knockdown would attenuate the DN injury in experimental diabetic nephropathy induced by streptozotocin (STZ). The sieving method was used to generate primary cultures of rat podocytes, and cultured according to the previous reports. The clinical data were analyzed for vein specimens from ESRD. Real-time quantitative PCR was used to examine the mRNA levels. Immuno-fluorescence assay was used for primary podocyte in vitro. Lectrophoretic mobility shift assay was used for DNA binding activity of NF-κB. HE staining for histological examination and western blot assay for protein expression were employed. The average GBM thickness (GBMT) was measured By using the electron microscopy. In vitro, MST1 level increased significantly in primary rat podocyte cultured in hyperglycemia condition. In vivo experiment, diabetes induced by a single STZ injection (50 mg/kg) in SD rats. Knockdown of MST1 expression by lentiviral mediated gene transfer partly reduced the proteinuria and the level of FASL, and improved the pathological changes of the diabetic kidney. In conclusion, the MST1 could be involved in DN pathogenesis and may serve as the target for development of new therapies for DN.

Keywords: Mammalian sterile 20-like kinase 1, podocyte, diabetic nephropathy

Introduction

Diabetic nephropathy (DN) is the leading cause of end-stage renal disease (ESRD) in the world. DN always be characterized by extra-cellular matrix (ECM) accumulation, glomerular basement membrane (GBM) thickening and podocyte apoptosis. Various abnormal signaling pathways, such as FAS/FASL [1], involve in the podocyte apoptosis. However, no universally accepted up-stream regulation pathways over such pathways has been found, and no universally accepted treatment strategy can prevent cell apoptosis under diabetic condition. Therefore, the study focused on mechanism of apoptosis in DN has been urgently needed.

The previous studies reported that some of the inflammatory cells, such as macrophages, dendritic cells, lymphocytes and non-immune cells, involve in the pathology of DN [2]. The inflammatory cells, such as nuclear factor-κB (NF-κB), tumor necrosis factor-α (TNF-α) and IL-6, have been implicated in diverse pathogenic pathways related to DN [3, 4]. Among the inflammatory cells, the macrophages are considered to be the most important immune cells infiltrating the diabetic kidney and cause the development of the renal damage [5]. In the processes of diabetic kidney, macrophages activated by various diabetic milieu elements, and release the proinflammatory cytokines, such as NF-κB, TNF-α and IL-6. All of the above cytokines could cause the injury to podocytes and tubular cells [6, 7]. Therefore, in this study, we preliminarily investigated the role of inflammatory cytokine, NF-κB, in the development of diabetic nephropathy.

Recently, mammalian sterile 20-like kinase (MST1) has been discovered, and which is a

487-amino-acid protein with a predicted molecular mass of 55.7 kDa [8]. The MST1 has been also involved in the apoptosis in many pathological disorders. Under normal condition, MST1 has been blocked as inactivated state in cytoplasm. It is strongly suggested that MST1 can be activated by various pro-apoptosis stimuli via caspase-3 cleaving and resulting in translocation into the nucleus, where it promotes chromatin condensation and induced apoptosis [9].

Interestingly, in addition to the important role in tumorgenesis [10], MST1 also involves in mechanisms of metabolic diseases and cardiovascular diseases. *Ardestani et al.* [11] found that MST1 could be a key mediator of apoptotic signaling for beta cell dysfunction under hyperglycemia. Meanwhile, *Odashima M et al*. [12] also found that endogenous MST1 plays an important role in mediating cardiac dilation, apoptosis, fibrosis, and cardiac dysfunction after the myocardial infarction (MI).

FAS/FASL pathway also called CD95/CD95L pathway [13], which is a member of the TNF-receptor super-family. This receptor contains a death domain. It has been shown to play a central role in the physiological regulation of apoptosis, such as DN [1]. Interestingly, some studies have shown that there could be a positive feedback loop involving MST1, and is possibly the caspase-3 and FAS/FASL pathways, which serves to amplify the apoptotic response [14]. We hypothesized that MST1 is an initiating trigger of apoptosis pathway, such as FAS/FASL pathway. The MST1 knockdown significantly restored renal function and decreased proteinuria level. Therefore, we will try to investigate differential expression of MST1 and its downstream regulatory network under hyperglycemia. The above descriptions provided the evidence that MST1 pathway could be fundamental novel target for DN.

Materials and methods

Experimental animals

Male Sprague-Dawley rats (purchased from the Experimental Animal Center of southwest medical university) weighing 200 to 250 g at the outset of the study were used. Animals were fed standard rat chow at 22°C to 24°C. Randomly, 54 rats were divided to 3 groups, including group A (normal control; n=18), group B (diabetes model + empty control lentiviral vector, n=18) and group C (diabetes model + MST1 ShRNA lentiviral vector, n=18). In group B and group C, diabetes was induced by Single IV injection of streptozotocin (STZ; purchased from Sigma, category reference: S0130) as we described before [15]. In group A, rats were received an equivalent volume of citrate buffer injection alone. Diabetes was defined as glucose levels 16.7 mmol/L at the end of 48th hour [15] following the injection. At the end of the 4th, 8th, and 12th week after modeling, 6 rats were sacrificed randomly from each group. All rats were fed the same diet and water. Insulin was not given to any of the animals. Blood and urine samples were collected and tested for glucose, serum creatinine (Scr) and 24-hour urine protein. This study was performed according to the Nation Institute of Health (NIH) Guide for the Care and Use of Laboratory Animal and approved by the institutional Animal Ethics Committee of southwest medical university.

Primary podocyte culture

To generate primary cultures of rat podocytes, sieving method was used in our study. The approximate method was used in pervious study in other group [16]. Glomeruli were isolated form Male Sprague-Dawley rats (weighing 100 to 120 g, purchased from the Experimental Animal Center of southwest medical university). Renal cortical tissue homogenates were carefully passed though a 150-mesh sieve and then a 200-mesh sieve. The isolated glomeruli were collected from the 200-mesh sieve. Then the isolated glomeruli were plated in 75 cm square culture flask that contained DEME-F12 (purchased from Gibco, USA; category reference: 12400-024) medium supplement with 10% fetal bovine serum (FBS, purchased from Bibco, USA; category reference: 16000-044) and 1% ITS (purchased from Gibco, USA; category reference: 51300-044) for 5 days. The primary outgrowing epithelial cells were trypsinized and passed through the 200-mesh sieve to remove the remaining glomerular cores. Then, the cells were cultured in DEME-F12 medium supplement with 10% FBS. Proliferating cells in confluence were sub-cultured after detachment with 0.25% trypsin in PBS. Then the cells were subcultured in two-chamber slides or six-well plastic plates coated with type I collagen. Cells were

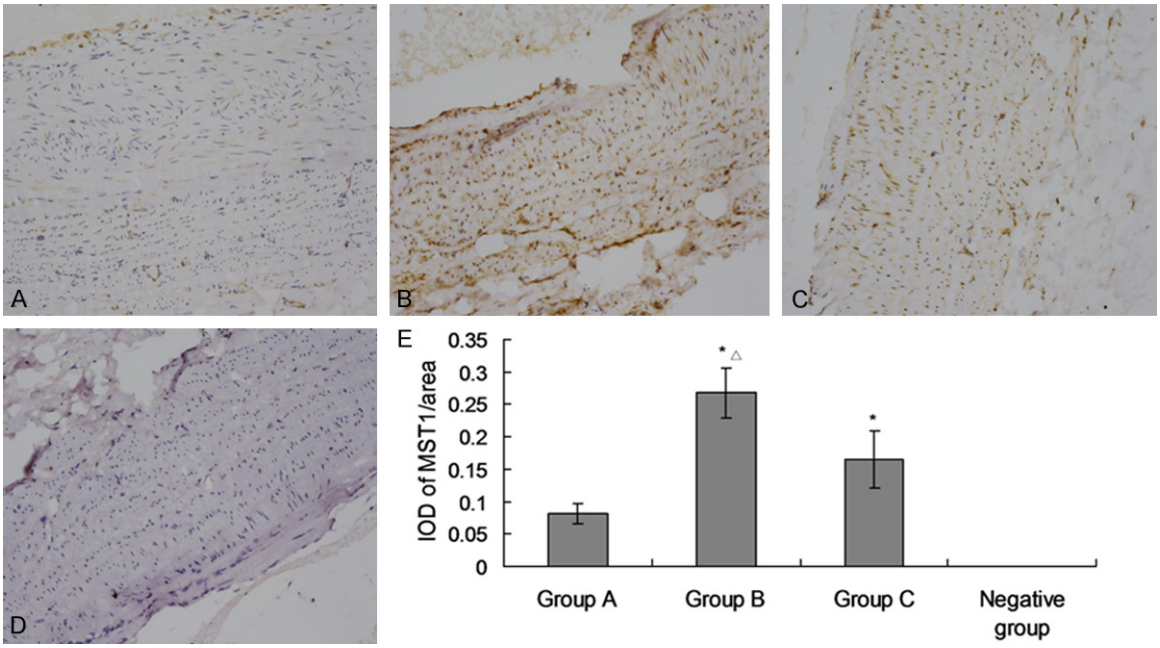

Figure 1. MST1 immunohistochemical staining analysis for vein specimens from ESRD. All patients were divided into 3 groups according to medical history: group A (normal control); group B (ESRD with diabetes) and group C (ESRD induced by NDRD). A: Normal control; B: Vein specimens from ESRD with diabetes; C: Vein specimens from ESRD induced by NDRD; D: Negative control, for negative control, the buffer replaced the primary antibody. E: Mean ratio of integral optical density to area was used in our study. For this data, it was shown that the level of MST1 in specimens from ESRD could be significantly higher than normal control and vein specimens from ESRD induced by NDRD. $^{*}P<0.05$ versus group A; $^{\Delta}P<0.05$ versus group C.

confirmed by both rabbit polyclonal anti-WT-1 protein and anti-Nephrin protein (purchased from Abcam, USA; category reference: ab58968) which are exclusively expressed by podocytes in the adult kidney. The purity of primary cells was measured by flow cytometry with rabbit Nephrin monoclonal antibody (purchased from Abcam, USA; category reference: ab72908).

After then, the cells were divided into 3 groups, including normal control (the concentration of glucose=5 mmol/L), Hyperglycemia group (cultured with hyperglycemia, the concentration of glucose=30 mmol/L) and Mannitol group. In order to mimic the osmolality change of the high glucose, we also designed a group which supplements with mannitol (Mannitol control group, concentration of mannitol=5 mmol/L). The end of 24th hour, 48th hour and 72th hour after cultured were considered as time points in our study.

The clinical data analysis for vein specimens from ESRD

Actually, the best clinical specimen for the study is the kidney tissue form DN case though renal biopsy. But in our hospital, there were a very small number of patients who received renal biopsy. Therefore, we failed to find the difference of MST1 expression between DN and normal control with kidney tissue from renal biopsy. Therefore, vein specimen from ESRD who received arteriovenous fistula operation with end to side anastomosis method.

According to principle of informed and consent, all patients whose vein specimen used in this study signed informed consent. All specimens were divided into 3 groups according to medical history, including group A (normal control), group B (ESRD with diabetes) and group C (ESRD induced by NDRD). Normal control got from great saphenous vein from trauma or bypass surgery. MST1 levels were examined by immuno-histochemical method with rabbit monoclonal antibody (purchased from Abcam, USA; category reference: ab124787) for all specimens.

Gene transfer

A lentiviral vector encoding rat MST1 shRNA (shMST1) and a control lentiviral vector encoding green fluorescent protein open reading

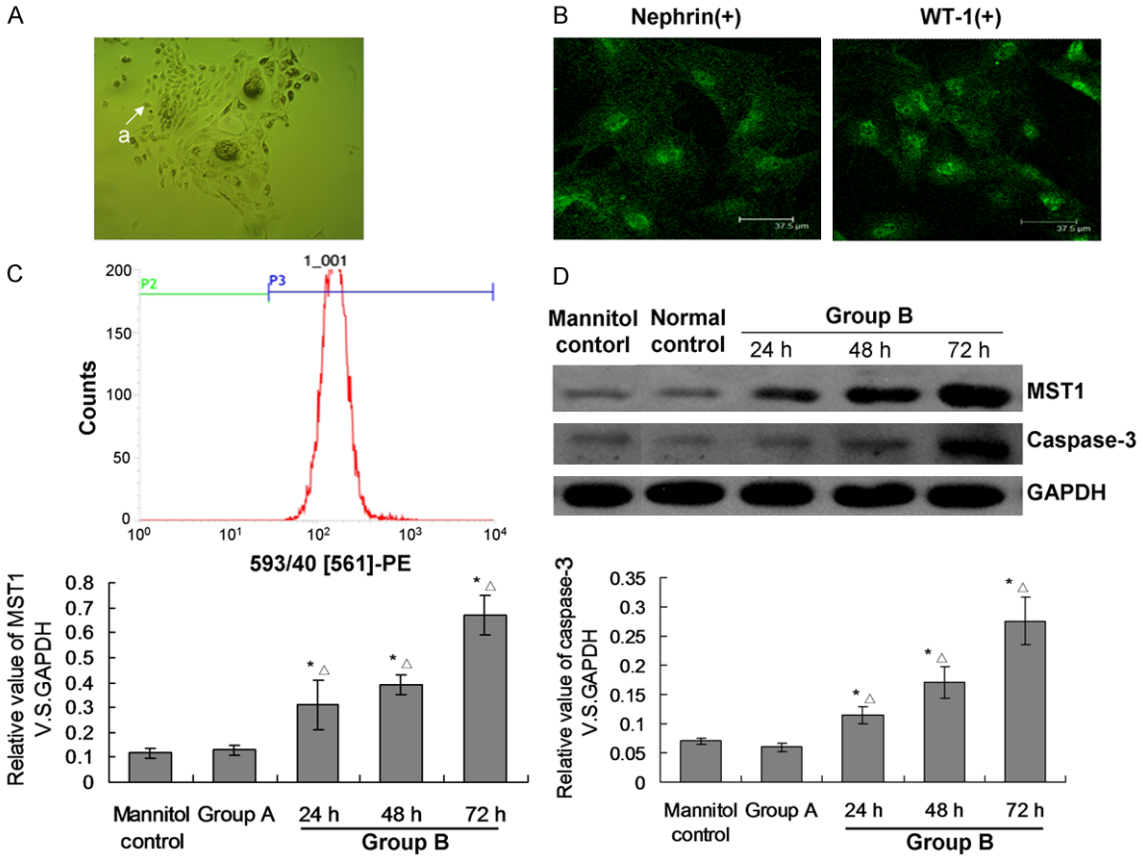

Figure 2. The analysis for primary podocyte in vitro. A. Primary podocyte was obveresed in microscope (×100), "a" represents the primary cell used for this study. B. The immunofluorescence stainings for Nephrin and WT-1 (with FITC, Green fluorescence) were performed in our study, only cells with Nephrin (+) and WT-1 (+) were used in our study. C. Flow cytometry for the cells with Nephrin (+). "a" represents cells with Nephrin (+) in P3 area. D. Western blot for MST1 and caspase-3 in vitro, the cells were divided into 3 groups, including group A (normal control, the concentration of glucose=5 mmol/L), group B (cultured with hyperglycemia, the concentration of glucose=30 mmol/L) and Mannitol control group (concentration of mannitol=5 mmol/L). $^{*}P<0.05$ versus normal control; $^{\Delta}P<0.05$ among group B.

frame (shGFP) were constructed by Western Biotechnology Ltd. Briefly, according the sequence of MST1 gene to design the premier and amplify the shRNA sequence. The vector LV3 was enzyme digested and purified, and linked to the shRNA sequence. Then, the linked LV3 and shRNA were transfected to the competent cells to produce the clone. The clone was identified by using the enzyme design method and gene sequencing assay to confirm the LV3-MST1-RNAi established successfully. The Lentiviral particles were produced in HK293T cells by co-transfecting system, including LV3-PG-p1-VSVG, PG-P2-REV and PG-P3-RRE. Virus titer was calculated by flow cytometry.

The rats were anesthetized with intramuscular injection of ketamine (35 mg/kg) and xylazine (5 mg/kg). As the report described previously (17), either shMST1 or shGFP solution at the title of 3×10^8 TU/ml was slowly injected from renal artery through acannula pre-implanted in the distal abdominal aorta. At the end of 7th day after gene transfer, the expression of MST1 was examined. Then, the rats were injected with either STZ (in group B and C) or citrate buffer (in group A). At the end of 1st week after gene transfer, all rats for each group were given vivo fluorescence imaging with Image Station In-Vivo FX system. At the end of 4th, 8th and 12th week after modeling, MST1 expression was evaluated in group A, B and C. MST1 shRNA Information shown as follow (mainly for the **Figures 3-5**): 5'-GATCC-(GN_{18})-(TTCAAGAGA)-(N_{18}C)-TTTTTTG-3'; 3'-G(CN18)-(AAGTTCTCT)-(N_{18}G)-AAAAAACTTAA-5'. The target sequence for MST1 was GCCGAGCCTTCCACTACAATA.

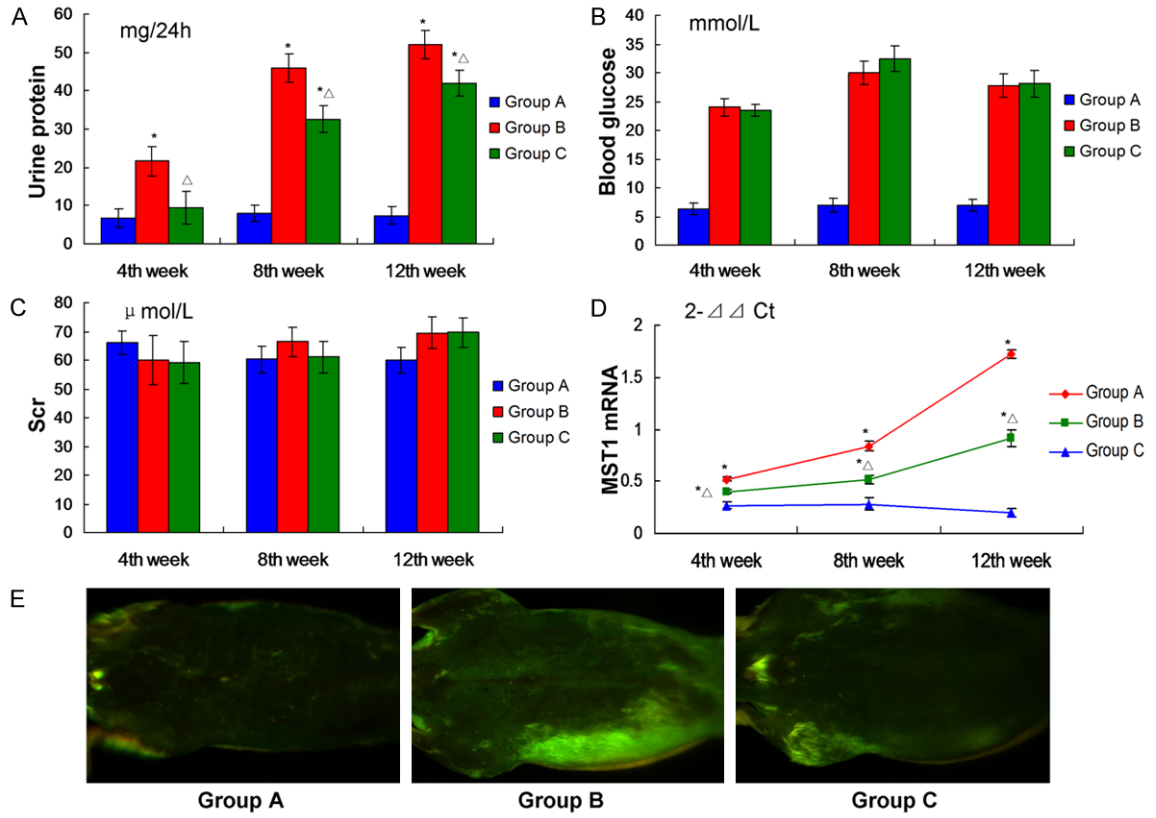

Figure 3. General finding for diabetic rats. All rats were divided to 3 groups, including group A (normal control), group B (diabetes model + empty control lentiviral vector) and group C (diabetes model + MST1 ShRNA lentiviral vector). A. The results of 24-hour urine protein. B. The results of glucose. C. The results of Scr. There was no significant difference among the 3 groups. D. RT-PCR results for MST1 mRNA. E. Vivo fluorescence imaging results: There were high intensities of green fluorescence in the rats in group B and group C due to lentiviral vector injection. $^{*}P<0.05$ versus group A; $^{\Delta}P<0.05$ versus group B at the same time point.

As described in the previous study [15], we used the MST1 monoclonal antibody which was diluted 1:100 at room temperature for the MST1 protein through envision technique. With pre-treating in citrate solution (pH 6.0) for 20 min and incubation with the primary antibody for 30 min, after which they were washed and incubated with Envision™ reagent (DAKO, UK; category reference: K5007) for 40 min. Envision™ reagent is a peroxidase-conjugated polymer backbone. In addition, Envision™ also carries secondary antibody molecules directed against rabbit and mouse IgG visualization with diaminobenzidine (DAB, Sigma, USA; category reference: D7679-1SET) and counterstained with Lillie's modified hematoxylin. We investigated the stained tissues using the same optical microscope setup (Olympus, CA, USA; category reference: BX15) and measured the optical density of stained MST1 using an image analysis system (Image pro plus, USA).

Real-time quantitative polymerase chain reaction

As described in previous study (17), RNA was extracted from the kidney tissues using TRIzol reagent (Invitrogen, USA; category reference: 15596-026) following the manufacturer's instructions. After DNase treatment (Promega, USA; category reference: M6101-1000), RNA was reversely transcribed into first strand cDNA using RevertAid™ First Strand cDNA Synthesis Kit (MBI, Fermentas, USA; catogery reference: K1611). Cycling and real-time PCR detection were performed using an ABI PRISM_7900 Sequence Detection System. Cycling conditions were listed as the followiings: 50°C for 2 min then 95°C for 10 min, followed by 35 cycles of 95°C for 30 s, 50°C for 45 s, and 72°C for 30 s. Gene-specific primers were designed using Vector NTI (Invitrogen, USA; category reference: 11.5.1), and the β-actin was used

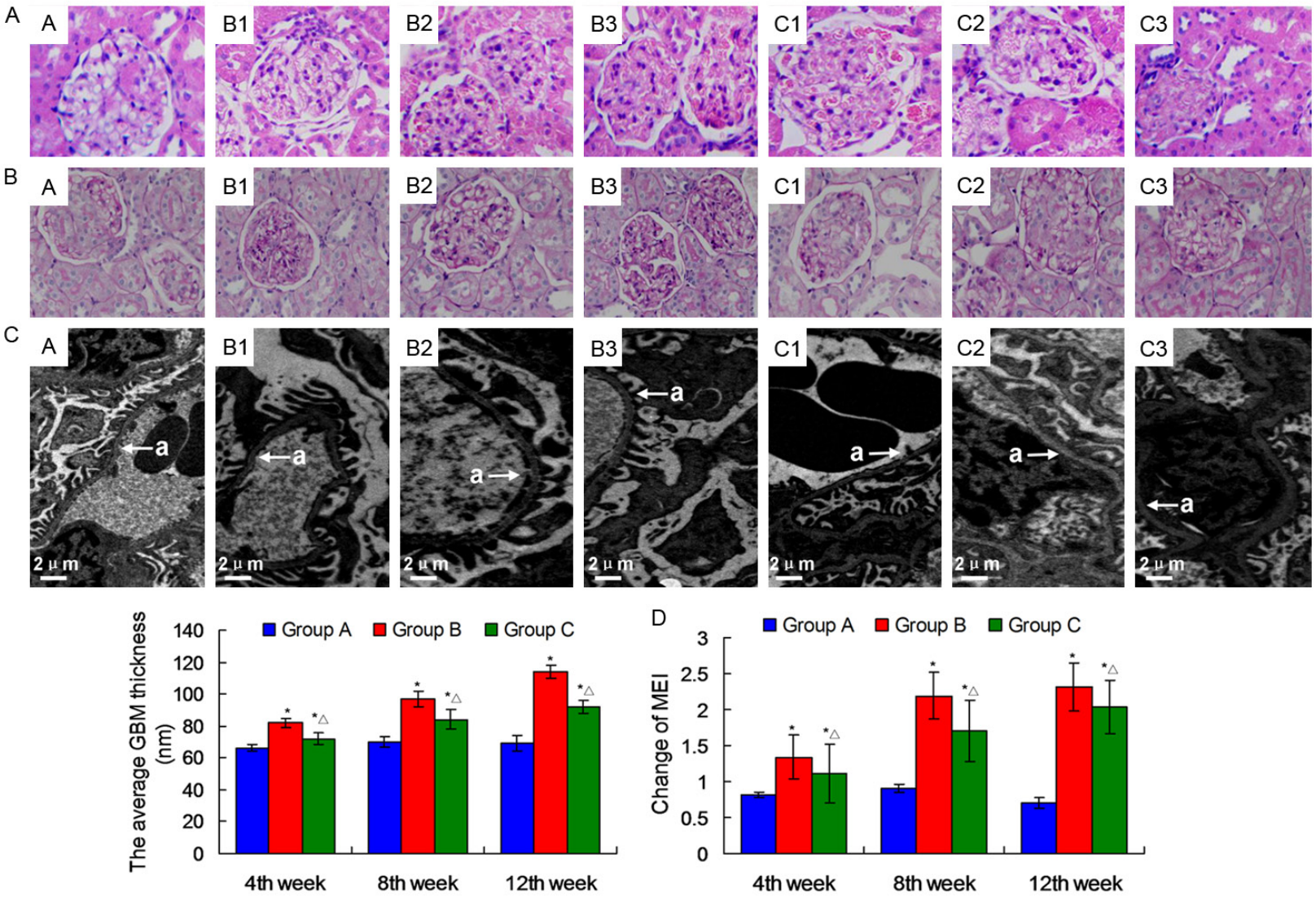

Figure 4. Pathological analysis in kidney tissue. A. The results of renal pathological with HE stain. B. The results of renal pathological with PAS stain. C. The results of renal pathological with Electron Microscopy. The GBM was thicker among the rats in groups B and C and was accompanied by fusion of podocytes. a: fusion of podocytes in our data. D. The change of MEI in rat renal tissue in our study. (A: the 4th week in group A; B1: the 4th week in group B; B2: the 8th week in group B; B3: the 12th week in group B; C1: the 4th week in group C; C2: the 8th week in group C; C3: the 12th week in group C). *$P<0.05$ versus group A; $^{\Delta}P<0.05$ versus group B at the same time point.

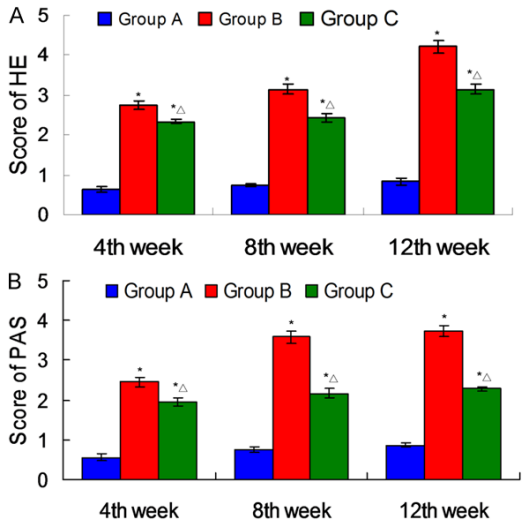

Figure 5. Pathological scores for the HE and PAS stain. A. Scores for the HE stain. B. Scores of the PAS stain. $^{*}P<0.05$ versus group A; $^{\Delta}P<0.05$ versus group B at the same time point.

as the internal control for normalization. The primer pairs for MST1 amplification were 5'-CACTCGCACCCTTTCCACC-3' (F) and 5'-CGACT CCCTCTTTG TGA-3' (R). The primers were 5'-CCCATCTATGAGGGTTACGC-3' (F) and 5'-TTTAATGTCACGCACGATTTC-3' (R) for β-actin. Transcription abundance was expressed as fold increase over the control gene calculated by the $2^{-\Delta\Delta Ct}$ method.

Immunofluorescence examine for primary podocyte in vitro

The primary cells were 4% formaldehyde fixed for 10 min and then incubated in 1% BSA/10% normal goat serum/0.3 M glycine in 0.1% PBS-Tween for 1 h to permeabilize the cells and block non-specific protein-protein interactions. Then, the cells were incubated with primary antibody (Rabbit polyclonal antibody to WT-1 purchased from Abcam, USA; Rabbit polyclonal antibody to Nephrin purchased from Abcam, USA; Rabbit monoclonal antibody to MST1 purchased from Abcam, USA) at 5 μg/ml overnight at 4°C. Goat Anti-Rabbit IgG H&L (Alexa Fluor® 647) or Goat Anti-Rabbit IgG H&L (FITC) at 1/150 dilution was used as the secondary antibody.

Electrophoretic mobility shift assay for DNA binding activity of NF-κB

An electrophoretic mobility shift assay (EMSA) for NF-κB binding to DNA was carried out with rats' kidney tissue. A nuclear extraction kit (purchased from Applygen, Beijing, China; category reference: OP-0002-1) was used to prepare nuclear extracts. Non-radioactive EMSA kit (purchased from Viagene Biotech Inc., USA; category reference: SIDET001) was used in shift assay. The binding reaction mixture contained 2 μL of nuclear extract, 1 μL of poly (dI-dC), biotin-labeled NF-κB probe in binding buffer (75 mM NaCl, 1.5 mM EDTA, 1.5 mM DTT, 7.5% glycerol, 1.5% NP-40, 15 mM Tris-HCl; pH 7.0). Samples were incubated for 30 min at 15°C in this mixture. DNA/protein complexes were separated from free DNA on a 6% non-denaturing polyacrylamide gel in 0.25 mM TBE buffer. The gel was transferred to a nylon membrane and detected by using streptavidin-HRP and chemiluminescent substrate. The following sequence (purchased from Western Biotechnology Inc, China) was used as a NF-κB consensus oligo: 5'-AGT TGA GGG GAC T TT CCC AGG C-3' and 3'-TCA ACT CCC CTG AAA GGG TCC G-5'.

Protocol for the histological examination of kidney tissue

Samples were isolated and embedded in paraffin to prepare 4-μm tissue slices that were investigated using hematoxylin and eosin (HE) staining and Periodic Acid-Schiff (PAS) staining, respectively. As described previously (18), mesangial expansion index (MEI) was assigned and scored in four levels from 0 to 3. With the index scores defined as the followings: 0, normal glomeruli; 1, matrix expansion occurred in up to 50% of a glomerulus; 2, matrix expansion occurred in 50 to 75% of a glomerulus; 3, matrix expansion occurred in 75 to 100% of a glomerulus. Scores were assigned for at least 30 glomeruli from kidney slices from each sample, and the means were calculated. Each slide was scored by a pathologist who was unaware of the experimental details.

Protocol for western blot in vivo and vitro

Using the western blotting method as previously described [15, 19], MST1 (cleaved MST1, clMST1), phospho-MST1/MST2 (phospho T183), FasL, Nephrin and Caspase-3 were examined. We used the rabbit monoclonal antibody to MST1 (Abcam, 1:500, USA; category reference: ab124787), rabbit polyclonal antibody to phospho-MST1/MST2 (Abcam, 1:500, USA; category reference: ab79199), rabbit

monoclonal antibody to caspase-3 (Abcam, UK, 1:500; category reference: ab32499), Rabbit polyclonal antibody to Fas Ligand (Abcam, 1:500, UK; category reference: ab15285) and rabbit monoclonal antibody to Nephrin (Abcam 1:500, UK; category reference: ab136894). Samples were homogenized in a radio-immunoprecipitation assay-lysis buffer containing 50 mM Tris-HCl, pH 7.4, 150 mM NaCl, 1% NP-40, 0.1% sodium dodecyl sulfate (SDS). Protein concentration was determined using the Bradford method and samples adjusted to equal concentrations. Samples were diluted with an equal volume of loading buffer and heated at 90°C for 5 min before being run on SDS-polyacrylamide gels. Electrophoresis was carried out in a Tris/glycine/SDS running buffer (25 mM Tris, 0.25 M glycin, 0.1% SDS). Following separation by electrophoresis, the proteins were transferred to polyvinylidene difluoride membrane (Siagma-Aldrich, USA; category reference: P4188). After transfer, the membranes were blocked in 5% non-fat milk in Tris-buffered saline (pH 7.4) supplemented with Tween 20 (TBST; 0.05%, v/v) for 1 h, before being probed with the following anti-rat antibodies in blocking solution overnight. Membranes were washed 3 times in TBST and then probed with peroxidase conjugated goat anti-rabbit IgG (1:5000; Nan Jing, Jin Site Biotechnology Co., China; category reference: 401315) for 1 h at 37°C. After washing, the specific signals were detected by enhanced chemiluminescence (Shinegene, Shanghai, Biotechnology Co., China; category reference: sc-350).

Electron microscopy

The average GBM thickness (GBMT) was measured from electron micrographs. The fractions of kidney tissue were fixed in 2% glutaraldehyde in 0.1 M sodium cacodylate, pH 7.4, 0.1 M sucrose, and 3 mM $CaCl_2$, at 4°C overnight, and centrifuged to a pellet. The pellet was rised in 0.15 M sodium cacodylate buffer containing 3 mM $CaCl_2$, pH 7.4 followed by postfixation in 2% osmium tetroxide, and 0.07 M sodium cacodylate buffer containing 1.5 mM $CaCl_2$, pH 7.4 at 4°C for 2 h. Sections were contrasted with uranyl acetate followed by lead citrate and examined in a Leo 906 transmission electron microscope at 80 kV. Digital images were taken using a Morada digital camera.

Statistical analyses

All values are expressed as means ± SEM. Multiple group means were compared by one-way ANOVA. The before and after within-group means were statistically evaluated using q tests. A value of $P<0.05$ was considered statistically significant. The SPSS 19.0 statistical software was used for analysis.

Results

The analysis for vein specimens from ESRD

To our knowledge, endothelial injury (20) and endothelial dysfunction [21] have been involved in pathogenesis of DN. On the other hand, some other vein endothelial cell line, for example, human umbilical vein endothelial cell line [22] has been used as an important sample in studies on DN. Furthermore, it has been shown that there could be characteristic differences and structural alterations in cephalic vein between diabetic and non-diabetic ESRD patients [23]. Therefore, we have tried to observe whether there could be a significant difference for MST1 expression in cephalic vein between diabetic and non-diabetic ESRD patients. Moreover, we also tried to find some supplementary evidence for the role of MST1 pathway in pathogenesis of DN.

The other clinical data of all patients shown in **Table 1**. In our data shown by immuno-histochemistry method, the levels of MST1 in both ESRD with diabetes and ESRD induced by NDRD were significantly higher than normal control *(P<0.05*). Compared with ESRD induced by NDRD, the level of MST1 in patients suffering from ESRD with diabetes was significantly higher *(P<0.05*). Meanwhile, the number of positively stained cells in tissue of ESRD with diabetes was significantly higher *(P<0.05*), which indicated there could be MST1 pathway activation in tissue (**Figure 1**).

The analysis for primary podocyte in vitro

WT-1 positive and Nephrin positive clones were selected and used for this study. It was measured by flow cytometry with rabbit Nephrin monoclonal antibody that the purity of primary cells could achieve to 95.12±2.37%. After cultured in hyperglycemia condition, compared with group A in vitro, the levels of caspase-3 and MST1 in group B increased from the end of 24^{th} hour after cultured in hyperglycemia condition. To our knowledge, this phenomenon has been reported in other cell line in response to pro-apoptotic factor [19], which indicated that caspase-3/MST1 pathway could be essential to trigger the apoptosis pathways (**Figure 2**).

Table 1. The clinical data for patients whose vein specimens enrolled in this study

	Group A (n=5)	Group B (n=12)	Group C (n=7)
Fmale/male	4:1	5:7	3:4
Average age	45.62±28.19	49.75 ±8.23	50.30±7.59
Glomerular filtration rate (ml/(min·1.73m^2))	98.24±6.15	4.43±3.02	5.02±2.44
Serum creatinine (umol/L)	65.15±21.33	913.25±67.15	976.67±82.70
Blood glucose (mmol/L)	4.65±0.76	11.27±7.12	6.09±2.41

All patients were divided into 3 groups according to medical history, including group A (normal control), group B (ESRD with diabetes) and group C (ESRD induced by NDRD). Glomerular filtration rate was calculated with MDRD formula (eGFR=175×[creatinine (mg/dl)]-1.234×[age (years old)]-0.179×sex (male=1, female=0.79)). All patients were given hemodialysis. Serum creatinine and blood glucose level were detected at the morning before hemodialysis.

Furthermore, there were no significant difference of the MST1 and caspase-3 level between the Group A and Mannitol control group (**Figure 2**). Therefore, we could confirm that the results were not due to the osmolality changes, but due to the high glucose treatment.

General finding for diabetic rats

At the end of 48th hour after modeling, blood glucose reached the standard for diabetic model in group B and group C in this study. And, they were also maintained at this level form the end of 4th week to the end of 12th week after modeling. Compared with group B, there was no significantly difference between group C and group B for blood glucose for each time points *(P>0.05*). The above results indicated that gene transfer treatment could not affect the level of blood glucose concentration.

The data of Scr was detected by automatic biochemical analyzer. It was shown that there was no significantly difference *(P>0.05*) for Scr among 3 groups. From the end of 4th week after modeling, the levels of 24-hour urine protein in group B and group C began to increase, whereas 24-hour urine protein in group C was not significantly different from group A *(P>0.05*) at the end of 4th week after modeling. Compared with group B, the levels of 24-hour urine protein in group C were significantly lower for each time points (**Figure 3**).

Detection of gene transfection

At the end of 1st week after gene transfection, the high levels of green fluorescent protein were found in rats of group B and group C by vivo fluorescence imaging, which was induced by lentiviral vector encoding green fluorescent protein open reading frame. Although increased gradually from the end of 4th week to 12th week after modeling both in group B and C, the level of MST1 in group C was significantly lower than the one in group B *(P<0.05*), which could be attributed to MST1 knockdown induced by gene transfection with MST1 ShRNA (**Figure 1**).

Pathological analysis in kidney tissue

There was no obvious pathological change observed in group A, The pathologic changes were not obvious in group B and C at end of 4th week after modeling. Since then, the pathological changes, including mesangial expansion, mesangial cell proliferation and glomerular hypertrophy, were found in group B and group C. The levels of MEI in group C were significantly lower compared to the one in group B for each time point *(P<0.05*). As revealed by PAS, glycogen content was also significantly different between group B and group C (**Figure 4**). Meanwhile, the scores of the HE stain and the PAS stain have also been calculated and listed in the **Figure 5**. The GBM was thicker among the rats in groups B and C and was accompanied by fusion of podocytes. These changes were significantly less common in the group C rats (**Figure 4**). The GBMT increased with time in group B and was markedly thicker than in the group C rats *(P<0.05*).

MST1 expression over time

To test how MST1 expression changed with time in our study, western blot analysis was performed on the kidney tissue. Due to up-regulation of MST1 with autophosphorylation (yielding MST1 phosphorylated on T183) [11], both the MST1, clMST1 and phosphorylation-MST1 levels were detected in our study. From the end of 4th week after modeling, both the MST1 and phosphorylation-MST1 levels in

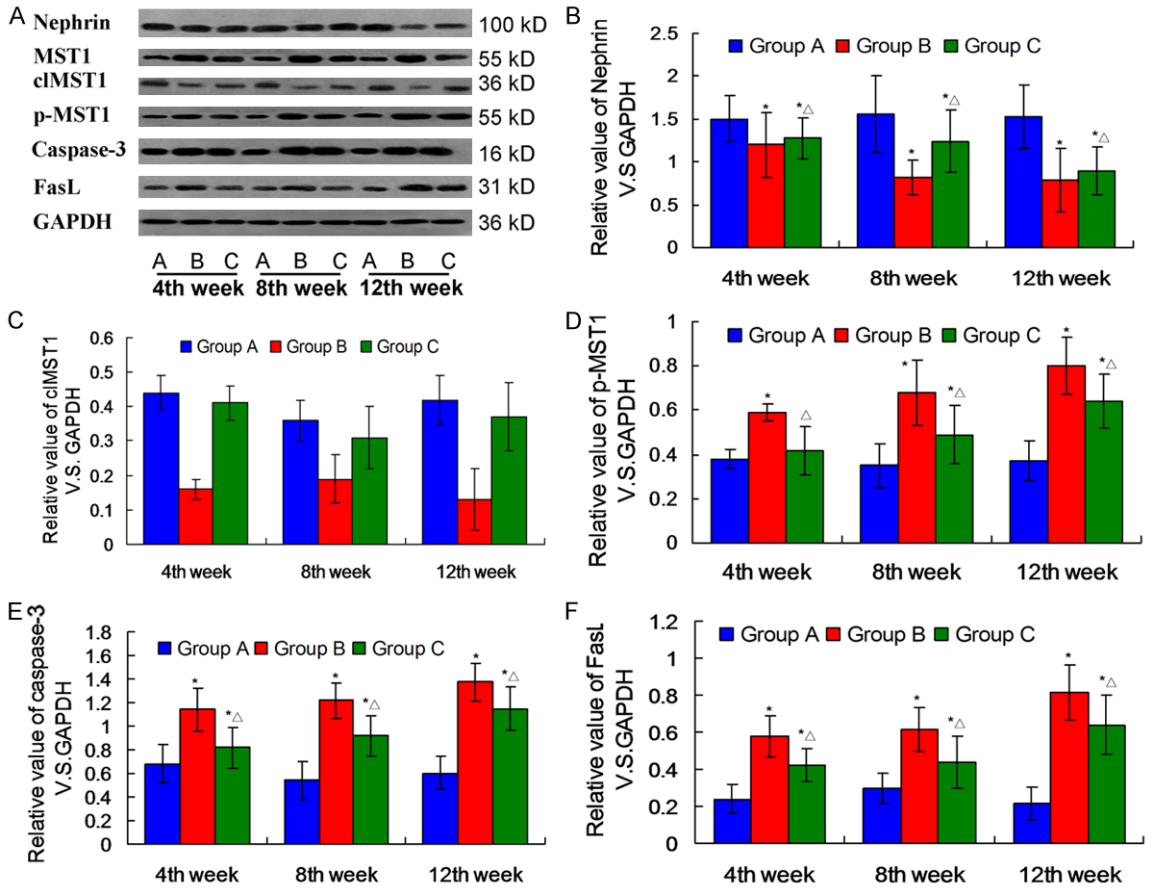

Figure 6. Western blot analysis in kidney tissue. A. Western blot assay examination for the proteins expression. B. Statistical analysis for the Nephrin expression. The "A" "B" "C" under the blot bands represent the Group A, B and C, respectively. C. Statistical analysis for the MST1 expression. D. Statistical analysis for the p-MST1 expression. E. Statistical analysis for the caspase-3 expression. F. Statistical analysis for the FasL expression. $^{*}P<0.05$ versus group A; $^{\Delta}P<0.05$ versus group B at the same time point.

group B and C increased significantly depend on time ($P<0.05$). Compared with group B, both the MST1 and phosphorylation-MST1 levels in group C were significantly lower for each time point ($P<0.05$). However, the clMST1 levels in group B was lower significantly compared to the group A and group C ($P<0.05$). It was shown by immuno-histochemistry that a low MST1 (full-length) expression could be observed in group A, mainly located in tubular epithelial cells. The MST1 (full-length) expressions in group B and C increased gradually. In the immuno-histochemistry assay, we used the antibody anti-full length MST1 (No appropriate anti-cleave MST1 was purchased), and the lower levels of full length MST1 represents the higher levels of cleaved MST1. Therefore, the clMST1 levels in group B was lower significantly compared to the group A and group C ($P<0.05$). Furthermore, the number of positive nuclei in group B and C increased significantly since the end of 4th week after modeling (**Figures 6** and **7**).

DNA binding activity of NF-κB in kidney tissue

NF-κB activation has been considered to play an important role in inflammation pathway [24], which could be involved in DN pathogenesis according to past study [25]. On the other hand, there could be some cross talk among Fas/FasL pathway and caspase-3 pathway [26]. Therefore, an electrophoretic mobility shift assay for DNA binding activity of NF-κB was performed. According to the data in this study, the level of NF-κB activation in group B and C significantly increased from the end of 4th week to 12th week after modeling ($P<0.05$). Compared with group B, the level of NF-κB activation in

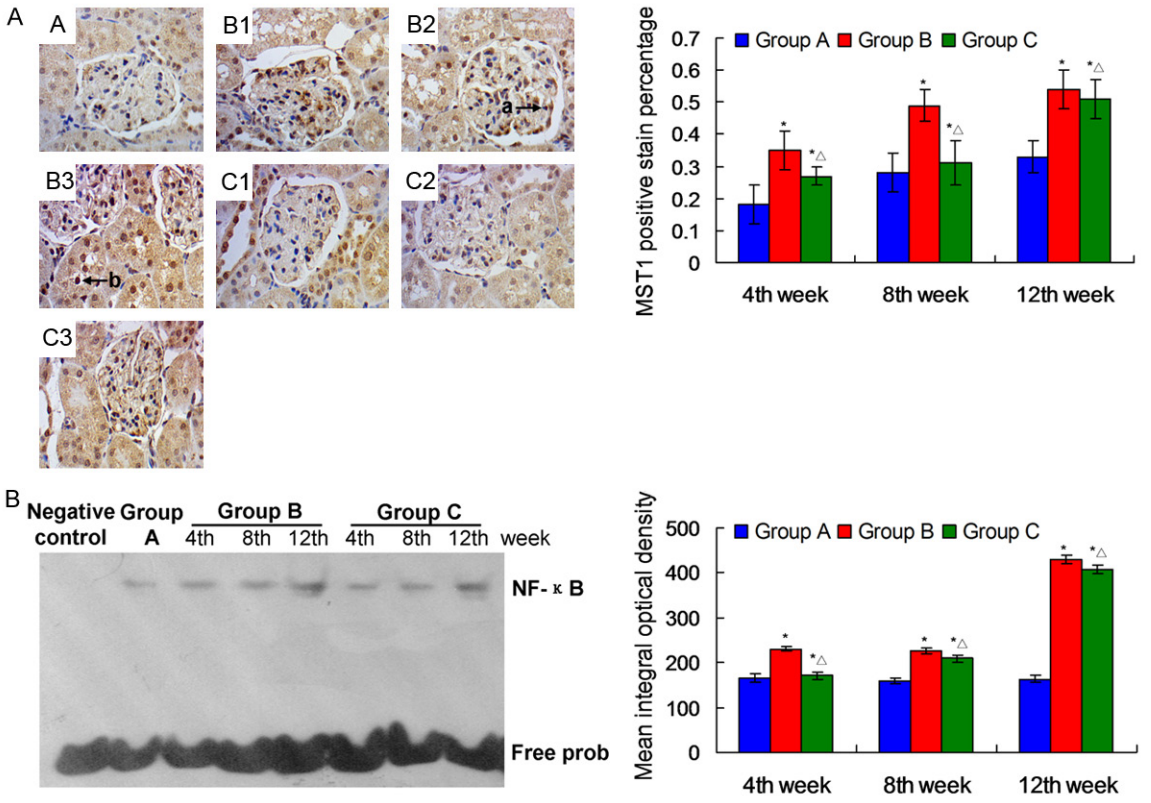

Figure 7. Immunohistochemical staining for MST1 and DNA binding activity of NF-κB in kidney tissue. A. Immunohistochemical staining analysis for MST1 level in rats. Mean ratio of integral optical density to area was used in our study. a: MST1 positive region in glomerular. b: Positive nuclei in renal tubular endothelial cells. It was illustrated that the level of MST1 could increase in group B and Group C. B. DNA binding activity of NF-κB in kidney tissue. Mean integral optical density (IOD) was used in our study for DNA binding activity of NF-κB analysis. (A: the 4th week in group A; B1: the 4th week in group B; B2: the 8th week in group B; B3: the 12th week in group B; C1: the 4th week in group C; C2: the 8th week in group C; C3: the 12th week in group C). *$P<0.05$ versus group A; $^{\Delta}P<0.05$ versus group B at the same time point.

group C was significantly lower for each time point *($P<0.05$*, **Figure 7**).

Nephrin and caspase-3 expression in rats' kidney tissue

AS we mentioned above, caspase-3 is a very important factor for MST1 pathway. On the other hand, Nephrin is essential for the maintenance of the function of podocyte [27]. Therefore, western blot analysis for Nephrin and caspase-3 were performed. The levels of Nephrin in group B and C gradually decreased since the end of 4th week after modeling and got drunk at the end of 12th week after modeling *($P<0.05$)*. The levels of caspase-3 in group B and C gradually increased since the end of 4th week after modeling and got peak value at the end of 12th week in this study. Compared with group B, the level of Nephrin in group C was significantly higher in each time point since the end of 4th week after modeling *($P<0.05$)*. The level of caspase-3 in group C was significantly lower in each time point since the end of 4th week after modeling *($P<0.05$)* (**Figure 6**).

FasL expression in rats' kidney tissue

To test how FasL expression changed with time in our study, western blot analysis was performed on the kidney tissue. The levels of FasL in group B and C gradually increased since the end of 4th week after modeling and got peak value at the end of 12th week in this study *($P<0.05$)*. Compared with group B, The level of FasL in group C was significantly lower in each time point since the end of 4th week after modeling *($P<0.05$)* (**Figure 6**).

Discussion

Our results showed the following mian points, indlucing ① there were significant increasing

for MST1 expression in both primary podocyte in vitro and cephalic vein specimens from ESRD; ② MST1 knockdown with lentiviral vector in diabetic rats could ameliorate clinical parameters indicative of DN (such as GBMT, MEI and 24-hour urine protein), and increase Nephrin expression, decrease caspase-3, Nf-kappa B and FasL level.

MST1 is core components in Hippo pathway which could be involved in cell proliferation, cell death and cell differentiation to regulate tissue growth control in mammals [10, 28]. Beside MST1, the core of the Hippo pathway consists Mammalian Sterile 20-like kinase 2 (MST2) which has been considered as homodimer of MST1 [29], the large tumor suppressor 1/2 serine/threonine protein kinases (LATS1/2), members of the AGC kinase family as well as their adaptor proteins Salvador (SAV; also termed WW45) and Mps-one binder 1 (MOB1) [30, 31]. MST1 is a target and activator of caspases, serving to amplify the apoptotic signaling pathway [11]. Thr 183 which was considered into our study for detection is an important phosphorylation sites for MST1 activation [11]. MST1 activation could trigger cell death though multiple downstream signaling pathways such as Sirtuin 1 [32], c-Jun N-terminal kinase pathway (JNK) [33], Caspase-3, phosphorylated histone H2B [34] and Fas/FasL pathway [20], whose consistent feature in all tested cell types is its proteolytic cleavage by caspase-3, in response to apoptotic stimuli, to a 34 to 36 kDa product [35].

As we mentioned above [11, 12], MST1 plays an important role in metabolic diseases and cardiovascular diseases. In our work, it was reported that there could be a significant increasing for MST1 expression in both primary podocyte in vitro and cephalic vein specimens from ESRD. These data indicated that MST1 pathway activation may exist in such condition. With both vein specimens from ESRD and primary podocyte, we significant increasing for MST1 expression under hyperglycemia condition. These results indicated that MST1 pathway activation also exists in diabetes. However, vein specimens form ESRD induced by NDRD were found a significant higher than normal control also that could be explained by uremic toxins. Possibly, MST1 expression could be affected by oxidative stress [36] induced by uremic toxins, although the mechanism is still unknown. By extension, there could be more opportunities for MST1 activation in hyperglycemia condition as well as endothelial dysfunction [21].

In this study, we also evaluated the renal function via staining the glomerulus by using the HE staining and the PAS staining method. The PAS staining results identified the dysfunction or abnormal of the kidney may be caused by the RAS activation. The RAS activation was manifested as increased levels of Ang II in the plasma and kidney, and increased the levels of renal renin, AT1R and AGT expression. Following, the above increased protein may be damage the renal function. In this study, the shRNA for MST1 could knockdown the effects of the diabetic nephropathy, and plays the protective role in the 4^{th} week, continue to the 12^{th} week with small changes.

In line with our data, *Mst1* ablation *in vivo* resulted in resistance to apoptosis induced by tumor necrosis factor-α, Fas ligand or IFN-γ [11], which could support our data in our study. As shown in some cell line cultured in H_2O_2 [37], oxidative stress could up-regulate MST1 expression. On the other hand, oxidative stress has emerged as a critical pathogenic process in the development of DN [17]. Based on these data, MST1 could be triggered by oxidative stress in DN, although the potential correlation between oxidative stress and MST1 activation in DN remains largely unexplored.

Our study confirmed that Neprin loss under hyperglycemia could be ameliorated by MST1 knockdown, combined with the data in primary podocyte in vitro, indicated that MST1 knockdown could be a protective role in podocyte under hyperglycemia. With a great possibility, MST1 knockdown could protect podocyte from apoptosis which is one of the typical characteristics of DN.

Ardestani A et al. [11] found that MST1 deficiency improves beta cell survival and function in vitro. However, no significant differences in serum glucose were observed between group B and group C. This phenomenon can be explained by the following points: ① the efficiency of MST1 knockdown in our study is not enough for beta cell, the knock not animal model (such as the model used in Lu L *et al.* [38] study) will be needed in further study; ② a variety of pathway could be involved in beta cell induced by STZ, thus, MST1 knockdown alone

could not shown a significant effect on glucose metabolism.

To our knowledge, the experimental results are optimistic, but whether the protective effect of MST1 on kidney is only through Fas/fasL under hyperglycemia is still unknown. For example, the interaction between MST1 and JNK pathway [39, 40], or interaction between MST1 and phosphorylated histone H2B [11, 33] under DN condition remains largely unexplored.

Admittedly, the current study has also some limitations as the following: ① the animal model used in this study is similar to type 1 diabetes, which is still a certain distance from type 2 diabetes in human. Therefore, the evidence to confirm the role of MST1 pathway in DN induced by type 2 diabetes has been not found; ② the efficiency of MST1 knockdown in our study is not enough, and MST1 shRNA in vivo gradually decayed over time, whereas DN develops slowly. The development of MST1 knockout animals will allow further extension of the present study; ③ to our knowledge, there is no standard antibody to detect phosphorylated MST1 (T183) alone. Therefore, we used polyclonal antibody to phospho-MST1/MST2 in our study. The development of new antibody is good for our further study; ④ the ample size of vein specimens was not enough. All patients enrolled in this study were Han nationality in china, came from southwest area of Sichuan Province. Therefore, there may be selective bias in our study. Study on a larger sample size will allow further extension of the present study.

In clinical practice, as well known, it is found that DN case could be more likely to develop chronic cardiovascular disease, and even sudden death. Combined with past study and our data [11, 12], this phenomenon can be explained by MST1 activation under diabetes condition partly. Therapeutic designed to knockdown MST1 activity in DN will needed in further.

Acknowledgements

National Natural Science Foundation of China (81200533); scientific research fund of Sichuan provincial health department (110356); scientific research fund of Luzhou medical college (ZRQN018, 2014ZD015) and scientific research fund of affiliated hospital of Luzhou Medical college (NO 2016-60).

Disclosure of conflict of interest

None.

Address correspondence to: Dr. Weihua Wu, Department of Nephrology, The Affiliated Hospital of Southwest Medical University, China. Tel: +86-013551660941; E-mail: wuweihuadcr@hainan.net

References

[1] Baba K, Minatoguchi S, Sano H, Kagawa T, Murata I, Takemura G, Hirano T, Ohashi H, Takemura M, Fujiwara T, Fujiwara H. Involvement of apoptosis in patients with diabetic nephropathy: A study on plasma soluble Fas levels and pathological findings. Nephrology (Carlton) 2004; 9: 94-99.

[2] Anders HJ, Banas B, Schlondorff D. Signaling danger: toll-like receptors and their potential roles in kidney disease. J Am Soc Nephrol 2004; 15: 854-67.

[3] Navarro-Gonzalez JF, Mora-Fernandez C, Muros de Fuentes M, Garcia-Perez J. Inflammatory molecules and pathways in the pathogenesis of diabetic nephropathy. Nat Rev Nephrol 2011; 7: 327-340.

[4] Lim AK, Tesch GH. Inflammation in diabetic nephropathy. Mediatros Inflamm 2012; 2012: 146154.

[5] You H, Gao T, Cooper TK, Brian Reeves W, Awad AS. Macrophages directly mediate diabetic renal injury. Am J Physiol Renal Physil. 2013; 305: F1719-27.

[6] Navarro-Gonzalez JF, Jarque A, Muros M, Mora C, Garcia J. Tumor necrosis factor-alpha as a therapeutic target for diabetic nephropathy. Cytokine Growth Factor Rev 2009; 20: 165-173.

[7] Shanmugam N, Reddy MA, Guha M, Natarajan R. High glucose-induced expression of proinflammatory cytokine and chemokine genes in monocytic cells. Diabetes 2003; 52: 1256-1264.

[8] de Souza PM, Lindsay MA. Mammalian Sterile20-like kinase 1 and the regulation of apoptosis. Biochem Soc Trans 2004; 32: 485-488.

[9] Ura S, Masuyama N, Graves JD, Gotoh Y. Caspase cleavage of MST1 promotes nuclear translocation and chromatin condensation. Proc Natl Acad Sci U S A 2001; 98: 10148-10153.

[10] Hong L, Cai Y, Jiang M, Zhou D, Chen L. The Hippo signaling pathway in liver regeneration and tumorigenesis. Acta Biochim Biophys Sin (Shanghai) 2015; 47: 46-52.

[11] Ardestani A, Paroni F, Azizi Z, Kaur S, Khobragade V, Yuan T, Frogne T, Tao W, Oberholzer J, Pattou F, Kerr Conte J, Maedler K. MST1 is a

key regulator of beta cell apoptosis and dysfunction in diabetes. Nat Med 2014; 20: 385-397.

[12] Odashima M, Usui S, Takagi H, Hong C, Liu J, Yokota M, Sadoshima J. Knockdown of endogenous MST1 prevents apoptosis and cardiac dysfunction without affecting cardiac hypertrophy after myocardial infarction. Circ Res 2007; 100: 1344-1352.

[13] Hadji A, Ceppi P, Murmann AE, Brockway S, Pattanayak A, Bhinder B, Hau A, De Chant S, Parimi V, Kolesza P, Richards J, Chandel N, Djaballah H, Peter ME. Death induced by CD95 or CD95 ligand elimination. Cell Rep 2014; 7: 208-222.

[14] Graves JD, Draves KE, Gotoh Y, Krebs EG, Clark EA, Both phosphorylation and caspase-mediated cleavage contribute to regulation of the Ste20-like protein kinase Mst1 during CD95/Fas-induced apoptosis. J Biol Chem 2001; 276: 14909-14915.

[15] Wu WH, Zhang MP, Zhang F, Liu F, Hu ZX, Hu QD, Yan XY, Huang SM. The role of programmed cell death in streptozotocin-induced early diabetic nephropathy. J Endocrinol Invest 2011; 34: e296-301.

[16] Chen CA, Hwang JC, Guh JY, Tsai JC, Chen HC. TGF-beta1 and integrin synergistically facilitate the differentiation of rat podocytes by increasing alpha-smooth muscle actin expression. Transl Res 2006; 148: 134-141.

[17] Tang WX, Wu WH, Zeng XX, Bo H, Huang SM. Early protective effect of mitofusion 2 overexpression in STZ-induced diabetic rat kidney. Endocrine 2012; 41: 236-247.

[18] Wu WH, Zhang MP, Yang SJ, Liu Q, Bai X, Qin JH, Peng B, Ou ST, Liu J, Zhao CY, Zhang Q, Hu QD, Xue L. Zhi-Long-Huo-Xue-Tong-Yu modulates mitochondrial fission through the ROCK1 pathway in mitochondrial dysfunction caused by streptozotocin-induced diabetic kidney injury. Genet Mol Res 2015; 14: 4593-4606.

[19] Zhang YJ, Lu CR, Cao Y, Luo Y, Bao RF, Yan S, Xue M, Zhu F, Wang Z, Duan LN. Imatinib induces H2AX phosphorylation and apoptosis in chronic myelogenous leukemia cells in vitro via caspase-3/Mst1 pathway. Acta Pharmacol Sin 2012; 33: 551-557.

[20] Maezawa Y, Takemoto M, Yokote K. Cell biology of diabetic nephropathy: Roles of endothelial cells, tubulointerstitial cells and podocytes. J Diabetes Investig 2015; 6: 3-15.

[21] Cheng H, Harris RC. Renal endothelial dysfunction in diabetic nephropathy. Cardiovasc Hematol Disord Drug Targets 2014; 14: 22-33.

[22] Wang C, George B, Chen S, Feng B, Li X, Chakrabarti S. Genotoxic stress and activation of novel DNA repair enzymes in human endothelial cells and in the retinas and kidneys of streptozotocin diabetic rats. Diabetes Metab Res Rev 2012; 28: 329-337.

[23] Hammes MS, Boghosian ME, Cassel KW, Funaki B, Coe FL. Characteristic differences in cephalic arch geometry for diabetic and non-diabetic ESRD patients. Nephrol Dial Transplant 2009; 24: 2190-2194.

[24] Yan R, Li Y, Zhang L, Xia N, Liu Q, Sun H, Guo H. Augmenter of liver regeneration attenuates inflammation of renal ischemia/reperfusion injury through the NF-kappa B pathway in rats. Int Urol Nephrol 2015; 47: 861-868.

[25] Zhou SJ, Bai L, Lv L, Chen R, Li CJ, Liu XY, Yu DM, Yu P. Liraglutide ameliorates renal injury in streptozotocin-induced diabetic rats by activating endothelial nitric oxide synthase activity via the downregulation of the nuclear factor-κB pathway. Mol Med Rep 2014; 10: 2587-2594

[26] Faouzi S, Burckhardt BE, Hanson JC, Campe CB, Schrum LW, Rippe RA, Maher JJ. Anti-Fas induces hepatic chemokines and promotes inflammation by an NF-kappa B-independent, caspase-3-dependent pathway. J Biol Chem 2001; 276: 49077-49082.

[27] Lin CL, Lee PH, Hsu YC, Lei CC, Chuang PC, Huang YT, Wang SY, Wu SL, Chen YS, Chiang WC, Reiser J, Wang FS. MicroRNA-29a promotion of nephrin acetylation ameliorates hyperglycemia-induced podocyte dysfunction. J Am Soc Nephrol 2014; 25: 1698-1709.

[28] Feng X, Chen Q, Gutkind JS. Oncotargeting G proteins: The Hippo in the room. Oncotarget 2014; 5: 10997-10999.

[29] Song H, Mak KK, Topol L, Yun K, Hu J, Garrett L, Chen Y, Park O, Chang J, Simpson RM, Wang CY, Gao B, Jiang J, Yang Y. Mammalian Mst1 and Mst2 kinases play essential roles in organ size control and tumor suppression. Proc Natl Acad Sci U S A 2010; 107: 1431-1436.

[30] Gomez M, Gomez V, Hergovich A. The Hippo pathway in disease and therapy: cancer and beyond. Clin Transl Med 2014; 3: 22.

[31] Oh S, Lee D, Kim T, Kim TS, Oh HJ, Hwang CY, Kong YY, Kwon KS, Lim DS. Crucial role for Mst1 and Mst2 kinases in early embryonic development of the mouse. Mol Cell Biol 2009; 29: 6309-6320.

[32] Yuan F, Xie Q, Wu J, Bai Y, Mao B, Dong Y, Bi W, Ji G, Tao W, Wang Y, Yuan Z. MST1 promotes apoptosis through regulating Sirt1-dependent p53 deacetylation. J Biol Chem 2011; 286: 6940-6945.

[33] Ura S, Nishina H, Gotoh Y, Katada T. Activation of the c-Jun N-terminal kinase pathway by MST1 is essential and sufficient for the induction of chromatin condensation during apoptosis. Mol Cell Biol 2007; 27: 5514-5522.

[34] Lu C, Shi Y, Luo Y, Duan L, Hou Y, Hu H, Wang Z, Xiang P. MAPKs and Mst1/Caspase-3 path-

ways contribute to H2B phosphorylation during UVB-induced apoptosis. Sci China Life Sci 2010; 53: 663-668

[35] Glantschnig H, Rodan GA, Reszka AA. Mapping of MST1 Kinase Sites of Phosphorylation. J Biol Chem 2002; 277: 42987-42996.

[36] Chae JS, Gil Hwang S, Lim DS, Choi EJ. Thioredoxin-1 functions as a molecular switch regulating the oxidative stress-induced activation of MST1. Free Radic Biol Med 2012; 53: 2335-2343.

[37] Xiao L, Chen D, Hu P, Wu J, Liu W, Zhao Y, Cao M, Fang Y, Bi W, Zheng Z, Ren J, Ji G, Wang Y, Yuan Z. The c-Abl-MST1 signaling pathway mediates oxidative stress-induced neuronal cell death. J Neurosci 2011; 31: 9611-9619.

[38] Lu L, Li Y, Kim SM, Bossuyt W, Liu P, Qiu Q, Wang Y, Halder G, Finegold MJ, Lee JS, Johnson RL. Hippo signaling is a potent in vivo growth and tumor suppressor pathway in the mammalian liver. Proc Natl Acad Sci U S A 2010; 107: 1437-1442.

[39] Graves JD, Gotoh Y, Draves KE, Ambrose D, Han DK, Wright M, Chernoff J, Clark EA, Krebs EG. Caspase-mediated activation and induction of apoptosis by the mammalian Ste20-like kinase Mst1. EMBO J 1998; 17: 2224-2234.

[40] Kakeya H, Onose R, Osada H. Caspase-mediated activation of a 36-kDa myelin basic protein kinase during anticancer drug-induced apoptosis. Cancer Res 1998; 58: 4888-4894.